Bulletin of Geography. Socio-economic Series, No. 68 (2025): 65-86
http://doi.org/10.12775/bgss-2025-0014

BULLETIN OF GEOGRAPHY. SOCIO–ECONOMIC SERIES

journal homepages:
https://apcz.umk.pl/BGSS/index
https://www.bulletinofgeography.umk.pl/

Integrating GIS and NetLogo-based modelling for simulating land-cover change scenarios in Mashhad Metropolitan Area, Iran

Sajedeh Baghban Khiabani[1], Mohammad Rahim Rahnama[2], Mohammad Ajza Shokouhi[3]

[1,2,3]*Ferdowsi University of Mashhad*, Department of Urban Planning in Geography, Mashhad, Iran, [1]e-mail: sajedeh.baghban@mail.um.ac.ir (*corresponding author*); [2]e-mail: rahnama@um.ac.ir, [2]https://orcid.org/0000-0002-4851-6327; [3]e-mail: shokouhim@um.ac.ir

How to cite:
Baghban Khiabani, S., Rahnama, M.R. & Ajza Shokouhi, M. (2025). Integrating GIS and NetLogo-based modelling for simulating land-cover change scenarios in Mashhad Metropolitan Area, Iran. *Bulletin of Geography. Socio-economic Series*, 68(68): 65-86. DOI: http://doi.org/10.12775/bgss-2025-0014

Abstract. This paper presents an agent-based model (ABM) integrated with GIS and NetLogo to simulate land-cover changes in the Mashhad Metropolitan Area (MMA) of Northeast Iran until 2030. It has two main objectives: first, to monitor land-cover changes from 2000 to 2020 using the Support Vector Machine (SVM) algorithm, which reveals an increase in built-up areas of 21,303 hectares (58.92%), alongside decreases in barren lands and green spaces of 15,922 hectares (25.73%) and 7,229 hectares (15.86%), respectively. Second, it conducts spatial simulations of land-cover changes projected for 2030 through the ABM in NetLogo, exploring four scenarios. Results indicate that Mashhad is expanding toward the north and west, with informal settlements encroaching on green spaces, while improved road access is expected to further accelerate urban land expansion.

Article details:
Received: 30 July 2024
Revised: 27 March 2025
Accepted: 15 May 2025

Key words:
land cover,
geography, planning & development,
Mashhad Metropolitan Area,
Support Vector Machine,
Agent-Based Modeling

Contents:

© 2025 (Sajedeh Baghban Khiabani, Mohammad Rahim Rahnama, Mohammad Ajza Shokouhi) This is an open access article licensed under the Creative Commons Attribution-NonCommercial License (http://creativecommons.org/licenses/by-nc/4.0/).

1. Introduction

Global urbanization has accelerated since the mid-20th century (Wang et al., 2023), with nearly 60% of the world's population expected to be living in urban areas by 2030 (Chen et al., 2023; Islam & Zannat, 2023). This urbanization, coupled with population growth, drives cities' spatial expansion, resulting in land-use/land-cover (LULC) changes that significantly impact the ecological environment (Kamran et al., 2023; Ritu et al., 2023). Land use (LU) pertains to human activities (e.g., agriculture, residential, commercial), whereas land cover (LC) describes the natural features of the land. Land use is frequently employed in planning and development studies, while land cover is primarily relevant in ecological and environmental research. These two concepts are often integrated in remote-sensing analyses to enhance understanding of environmental changes and human impacts on the landscape (Rayan et al., 2021).

LULC data changes are crucial for urban managers and policymakers to address the challenges of unplanned urbanization (Zarin & Zannat, 2023). The LULC changes have led to the loss and degradation of natural resources, reduced urban land use efficiency, increased deforestation and arable land loss, intensified land use, and increased environmental pollution. These issues threaten ecosystem sustainability, underscoring the need for assessment and management for sustainable development (Angel et al., 2011; Zhang et al., 2018; Wang et al., 2020; Zhao et al., 2022; Chen et al., 2023; Daams et al., 2023; Islam & Zannat, 2023).

In Iran, sustainable development has gained significance due to rapid development and environmental degradation, impacting local, regional and global conditions (Nuccy et al., 2016). Mashhad, Iran's second-largest city, has experienced unbalanced growth; its population surged from 1.5 million in 1990 to over three million by 2020. During this time, the city expanded from 7,800 hectares to 30,000 hectares, with 3,894 hectares in informal settlements, primarily in the north (Mashhad Municipality, 2020). This rapid growth has led to inefficient land use/land cover, environmental degradation, and other urban challenges (Motlaq & Abbaszadeh, 2012).

Additionally, the holy shrine of Imam Reza (AS) is central to Mashhad's development, attracting ~30 million pilgrims annually. Its presence drives significant physical and functional changes in the metropolitan area, with various policies implemented to leverage its touristic role (Teimouri et al., 2022).

Addressing the challenges faced by Mashhad requires a comprehensive study of (LULC) changes, not only in historical and current contexts but also projecting into the future. This approach is essential for enhancing urban sustainability, guiding urban expansion effectively, and safeguarding natural resources.

A thorough understanding of LULC changes in the Mashhad Metropolitan Area (MMA) will equip policymakers and urban planners with the insights needed to allocate spatial investments judiciously. By modeling these changes, planners can identify valid and reliable indicators that align with spatial objectives and inform decision-making processes (Coronese et al., 2023). Moreover, a well-structured LULC model that incorporates all relevant factors can foster a sustainable environment by facilitating appropriate land-use practices (Li et al., 2023; Motieyan & Mesgari, 2018). LULC modeling is a method to simulate land use/land cover and indicate the relations between LULC changes and surroundings (Liang et al., 2018).

Traditional LULC approaches have difficulties in effectively capturing land-use changes, surroundings and different agent dependencies (Park et al., 2011; Khan et al., 2017; Kucsicsa et al., 2018; Fu et al., 2018). Among LULC, Agent-Based Models (ABMs) could help improve this shortcoming and have higher efficiency than other kinds of modeling methods in examining the interactions of agents with each other and with the environment (Abar, 2017; Achter et al., 2023; Secchi et al., 2024). ABMs simplify the real world by decomposing a system into a set of agents (potentially heterogeneous) that interact with each other and with their environment (Beerman et al., 2023; Lang & Ertsen, 2023; De Visscher et al., 2024). This method enables the quantitative study of the behaviors of heterogeneous agents and their interactions over time (Dicks et al., 2024).

This study employs NetLogo as an Agent-Based Modeling (ABM) tool to investigate the dynamic relationships among agents, environmental factors and constraints. NetLogo is a versatile modeling environment for simulating natural and social phenomena, offering robust modeling, graphical and statistical capabilities, along with GIS support. Its extensive library of sample models and active user community contribute to its popularity as an ABM platform (Vahidi & Yan, 2014; Cenani, 2021; Lee et al., 2023; De Visscher, 2024). By employing a bottom-up rule-based approach with simple online updating for trading constraints, NetLogo's flexibility allows for effective interdisciplinary connections (Cao et al., 2023; Dicks et al., 2024).

To model LULC changes in NetLogo, accurate and consistent data regarding the urban environment and its changes are needed. For this purpose, technological advances such as satellite-based observations, and high-resolution remote-sensing (RS) imagery offer a cost-effective, consistent and accurate method to capture the details of urban dynamics and monitoring LULC changes (Huang et al., 2018; Zhao et al., 2020; de Souza Silva et al., 2023). There are numerous LULC classification algorithms; among them, Support Vector Machine (SVM) has emerged as an effective supervised classifier for LULC mapping using satellite imagery. Studies have shown that SVM outperforms other classifiers like Artificial Neural Networks (ANN) in terms of accuracy and reliability. It is effective in high-dimensional spaces, robust to overfitting, and provides clear separation margins between classes (Pham et al., 2019; Nehzak et al., 2020; Yousfi et al., 2022).

Numerous scholars have attempted to tackle the problems of urban LULC changes, and a wide variety of methods and approaches have been identified, making it particularly challenging. The methods used in different studies can be classified into the following: statistical methods (Park et al., 2011; Kucsicsa et al., 2018; Huang et al., 2019; Zhang et al., 2021), cellular automata models (Kamusoko et al., 2009; Wang et al., 2012; Liu et al., 2020; Rahnama, 2021), economic models (Irwin & Geoghegan, 2001; Koomen & Buurman, 2002; Walker, 2004), agent-based models (Karali et al., 2011; Motieyan & Mesgari, 2018; Li et al., 2019; Coronese et al., 2023), artificial neural networks (Dixon & Candade, 2008; Liu et al., 2020; Rahanama & Wyatt, 2021), and Markov chains (Han et al., 2015; Jenerette & Potere; 2020). Some researchers have applied hybrid approaches (Tayyebi & Pijanowski, 2014; Rahnama et al., 2021). ABMs have emerged as a powerful tool for simulating LULC changes at various scales. These models can capture complex human–environment interactions and individual decision-making processes in agricultural and urban landscapes (Innocenti et al., 2019; Li et al., 2024). ABMs are often combined with other approaches, such as cellular automata, spatial logistic regression or Markov models, to enhance their predictive capabilities and address specific research questions (Li et al., 2024). While ABMs have traditionally been applied at local scales, recent efforts have extended their use to regional-scale analyses (Valbuena et al., 2010). These models can simulate various land-use processes, including farm cessation, expansion and diversification, as well as urban development and agricultural land conversion (Valbuena et al., 2010; Innocenti et al., 2019). Despite their potential, challenges remain in applying ABMs to large-scale modeling and fully capturing the complexity of agricultural land systems (Yu et al., 2013).

The evaluation of existing research reveals a lack of focus on metropolitan areas (i.e., Melbourne, Tehran, Tokyo) facing similar challenges (i.e., the loss of green spaces, the development of the built-up regions, and subsequent development of the urban area), particularly in the interconnected dynamics between central cities and surrounding population centers. This study addresses this gap by examining the Mashhad Metropolitan Area (MMA) in Iran, which is densely populated and rapidly expanding. It aims to explore the dynamic relationships between land cover (LC), influencing agents and management factors. Unlike previous LULC models primarily relying on historical trends (Kamusoko et al., 2009; Wang et al., 2012; Han et al., 2015; Jenerette & Potere; 2020; Li et al., 2024), this research incorporates various natural and management factors to assess simulation outcomes. Additionally, a key feature of this study is its steerability, allowing users to pause and modify simulations to meet practical needs without worrying about the validity of changes.

There is a notable gap in research on integrating GIS and NetLogo for LULC analysis, despite its potential for high performance across various scales. Previous studies have mainly used ArcGIS to create urban maps, incorporating road networks and land-use data as base maps in NetLogo (Zhaka & Xhina, 2021). In contrast, this study aims to utilize GIS to provide geospatial data that constrain agent behavior, using land-cover maps from three different years, road networks, and topographic information. Unlike earlier research, which was limited in predicting diverse scenarios (Valbuena et al., 2010; Innocenti et al., 2019; Jenerette & Potere, 2020; Li et al., 2024), this model is adaptable to varying conditions and agent behaviors, allowing for the generation of multiple scenarios based on planners' and politicians' policies. Additionally, this research introduces a validation criterion that begins with modeling the current situation, validating the model and projecting future scenarios, thereby enhancing the robustness and reliability of the outcomes.

Addressing the gap identified in previous studies, this paper investigates urban LC changes in MMA between 2000 and 2020. It simulates change patterns up to 2030 within the 181,419 hectares, encompassing over three million residents and accommodating thirty million pilgrims annually. Recognizing that LULC models are essential for promoting sustainable urban development (Lai, 2023), this study proposes an advanced LC Agent-Based Model that includes policymakers, developers and households as key agents to optimize the shape and spatial patterns of land cover in MMA.

Given the area's large population, high tourist volume and industrial characteristics and the critical role of the metropolitan area in Iran and the Islamic world, any modeling effort must be adaptable and not constrained by linear processes. Therefore, this paper introduces a Progressive approach to LC modeling that integrates GIS with NetLogo as a programmable environment.

The integration of remote-sensing (RS) and GIS technologies has demonstrated effectiveness in modeling LC, with techniques like Support Vector Machines (SVMs) showing significant promise. Consequently, the necessary data for LC simulation in the study area are obtained using these advanced technologies and the SVM method, enhancing the model's accuracy and flexibility (Njoku & Tenenbaum, 2022).

In this paper, NetLogo simulates the LC in response to user-designed scenarios in the context of the existing natural and built environment and road network characteristics. Ideally, any new theory proposed by the user can link to other features, if necessary, and would be implemented as a distinct scenario.

2. Research materials and methods

2.1. Study area

The Mashhad Metropolitan Area (MMA), as the second-largest metropolis in Iran, exemplifies both the challenges and opportunities faced by urban environments due to its provincial centrality and the relationships between Iran and cities across Asia. Situated in north-eastern Iran, MMA extends from 59°3' to 60°35' east longitude and from 35°42' to 36°59' north latitude, encompassing 37,357 hectares within a total metropolitan area of 181,419 hectares. This region, with its concentration of industrial zones, connections to rail and air transport networks, and dynamic migration patterns, has become a model of land-cover (LC) change through agent-based modeling (ABM), offering valuable insights for other large cities facing similar developmental challenges. Renowned for its rich historical and cultural heritage, Mashhad attracts over three million tourists each year. It is also a significant industrial hub, positioning it as a critical destination for immigrants. The rapid advancement of the social economy, alongside continuous urbanization and industrial growth, has spurred a considerable expansion of construction in the region in recent years. As a result, Mashhad faces numerous ecological challenges, including land-cover changes.

MMA encompasses 177 rural settlements (Fig. 1). Among these, the cities of Torghabeh and Shandiz are particularly noteworthy, having both impacted and been influenced by their surroundings. The terrain features a mix of plains and hills; notably, the Binalud mountain range traverses the southern part of the area, significantly affecting the development of Torghabeh and Shandiz as prominent tourist destinations. Consequently, the agricultural lands in their vicinity are experiencing some of the most significant shifts in land use. Additionally, the Kashaf River, flowing north of Mashhad, creates a favorable environment for agricultural activities.

With the ongoing emergence of informal settlements in the north, planned expansions in the western part of the city, and rising immigration and population growth, it is imperative for the metropolitan area to pursue sustainable development strategies that minimize harm to its natural resources.

To model the LC changes in MMA and create related scenarios, this paper is structured as follows: 1) Remote-sensing data classification in GIS and 2) LC modeling and creating scenarios in NetLogo (Fig. 2).

2.2. Remote-sensing data classification

The remote-sensing technology provided a lot of information about geospatial changes in MMA, and Geographic Information Systems (GIS) tracked and categorized these alterations.

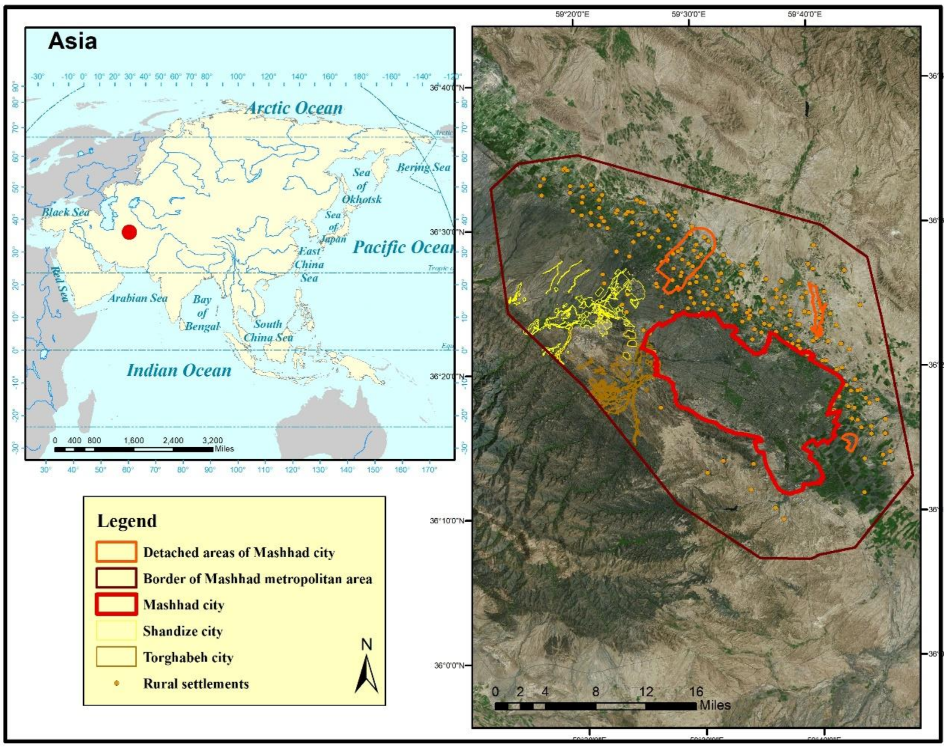

Fig. 1. Location of the study area
Source: research findings based on metropolitan vector data

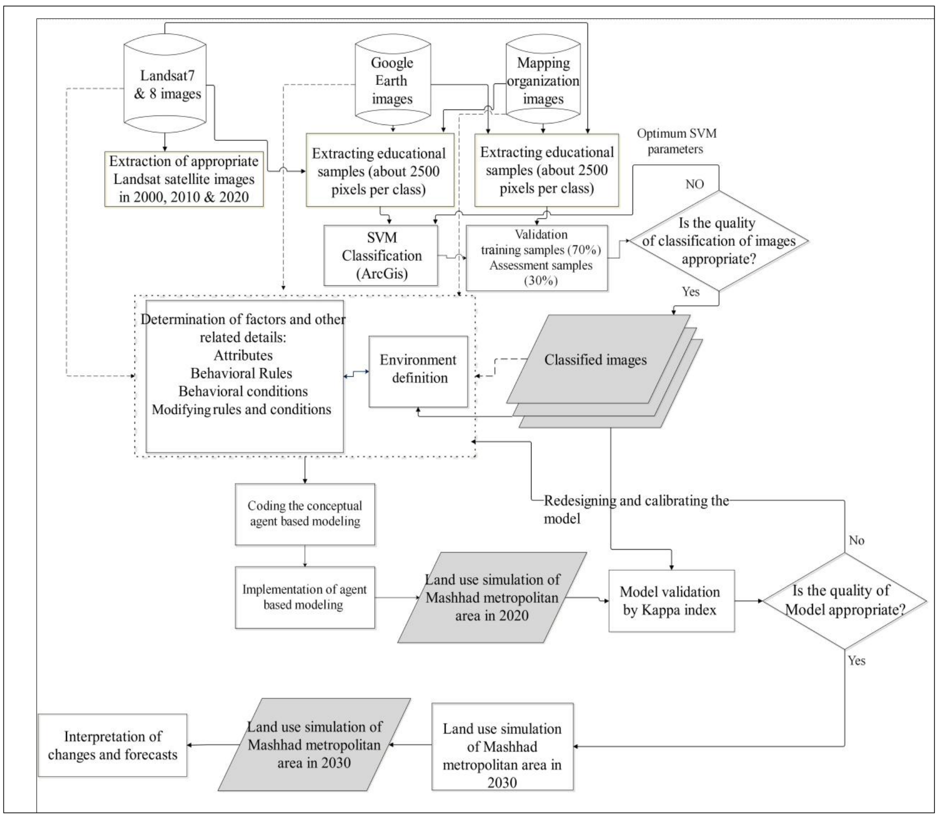

Fig. 2. Research flowchart
Source: research findings, 2023

2.2.1. Data source

The data used in this study include land-cover data, Digital Elevation Model (DEM), Landsat (7 and 8) remote-sensing data (because of their long historical record from 1999), and road-network data. Road-network data were obtained from the (https://www.openstreetmap.org/). The DEM is derived from the Geospatial Data Cloud (http://www.gscloud.cn) and Landsat remote-sensing data are obtained from the United States Geological Survey (https://earthexplorer.usgs.gov/). Landsat satellite images were collected for three sample years (2000, 2010, 2020). The imagery consisted of 2000 and 2010 Landsat 7 Enhanced Thematic Mapper (ETM), and 2020 Landsat 8 Operational Land Imager (OLI) sensor Surface Reflectance with a resolution of thirty meters. Finally, each image collection band (1,2,3,4,5,7) was composited.

2.2.2. Data classification by Support Vector Machine (SVM)

Several methods exist for satellite image classification, including traditional maximum likelihood, deep learning and various machine learning algorithms (Zhang & Li, 2014; Murmu & Biswas, 2015; Potic & Potic, 2017; Varamesh et al., 2017 Arabi Aliabad et al., 2019; Zeraatpisheh et al., 2019; Jijo & Abdulazeez, 2021; Razaque et al., 2021; Shivakumar, 2021). Among these, SVM, developed by Vapnik in 1995, stands out as a powerful tool for raster data management. SVM effectively identifies distinct classes while minimizing classification errors, making it a valuable method for satellite imagery analysis (Pham, 2019; Talukdar et al., 2020; Santarsiero et al., 2022). SVM is a non-parametric technique used in supervised learning algorithms, drawing from statistical learning theory for classification tasks. This method excels in handling large datasets and is versatile, adapting successfully for classification, regression, and outlier detection (Pham et al., 2019; Santarsiero et al., 2022). SVM models utilize a user-defined kernel function, which facilitates the transformation of nonlinear decision boundaries in the data into linear separations within a high-dimensional space (Jasim et al., 2024). This capability enhances the model's effectiveness in complex classification challenges. So, in this study, the SVM method is used to classify LC in the study area. To accomplish land-cover classification, ArcGIS provides a segmentation and classification tool that includes an SVM classifier for generating training data. Satellite images are imported into ArcMap, where various training sample features are identified across five LC classes: built-up areas, green spaces, barren lands, rocks, and water bodies.

After selecting the training samples, hyperparameters were optimized using a tuning technique. This method allows the software to automatically adjust hyperparameter values based on the number and complexity of the samples. These values can be re-evaluated after model validation and modified manually if necessary. A Gaussian kernel function was employed using hyperparameters with a gamma value of 32 and a C value of 8192. The high gamma value indicates that the kernel function fits the training data closely, enabling it to effectively capture the complexities of the data distribution. In contrast, the C parameter set to 8192 demonstrates a strong emphasis on minimizing training errors, resulting in a robust and precise decision boundary. This balance enhances the model's ability to accurately separate the classes. Overall, these hyperparameters have been specifically calibrated to optimize the classification efficiency and accuracy of the model in a complex region such as Mashhad.

Finally, LC classification was performed on the entire satellite image using the SVM algorithm based on the training dataset. The following classification calculated overall accuracy and the Kappa coefficient to validate the results. The overall classification accuracy – indicating the percentage of correctly classified cells – exceeded 90% in all three images. The minimum Kappa coefficient observed was 85%, which is considered nearly perfect for land-use classification (Varamesh et al., 2017), with values exceeding 90% for all three images. These results demonstrate that the classification validity of the images is strong.

2.2.3. Methodology of Agent-Based Modeling in NetLogo

In this study, we employed agent-based modeling (ABM) techniques using NetLogo software to analyze LC changes over the period from 2000 to 2020.

The modeling framework is based on a set of specific regulations that govern the interactions among various agents, as well as the relationships between agents and their environment, which includes the following components:

A. Regulations configuration

The regulations defined within the model dictate the behavior of agents and their interactions. These regulations are derived from a comprehensive analysis of historical land-cover changes within the study area. In our modeling approach, we distinguish between two types of regulations:

1) Constant Rules: These are the foundational regulations that remain unchanged across all simulation scenarios. They establish the basic framework for agent interactions (Table 1).

2) Variable Conditions: These refer to the parameters that can be adjusted in each simulation run. By modifying these conditions, we observe how changes affect the outcomes of the model (Table 2).

B. Framework development

The derived framework for the agent-based model draws upon historical trends of land-cover changes from 2000 to 2020. This framework allows us to simulate various scenarios by maintaining fixed rules while altering the conditions.

For model implementation, rules are consistently applied across all scenarios, ensuring a stable baseline for comparison (Table 1). The most important aspect of NetLogo in this research is the application of these rules.

Conditions (Table 2): The numeric values for conditions are systematically varied across different scenarios, enabling the exploration of multiple outcomes based on specific parameter adjustments.

2.3. LC modeling and creating scenarios in NetLogo

The simulation is implemented in NetLogo, a programming language and agent-based simulation environment (Fig. 4). It is particularly well suited for modeling complex systems developing over time. Modelers can give instructions to thousands of “agents” all operating independently. This makes

Table 1. Rules governing land-cover changes from 2000 to 2010 and from 2010 to 2020

	Rules
1	Built-up areas developed on a slope of 0 to 15%.
2	Built-up areas developed adjacent to roads.
3	Cell development spreads from the vicinity of pre-developed cells.

Source: research findings, 2023

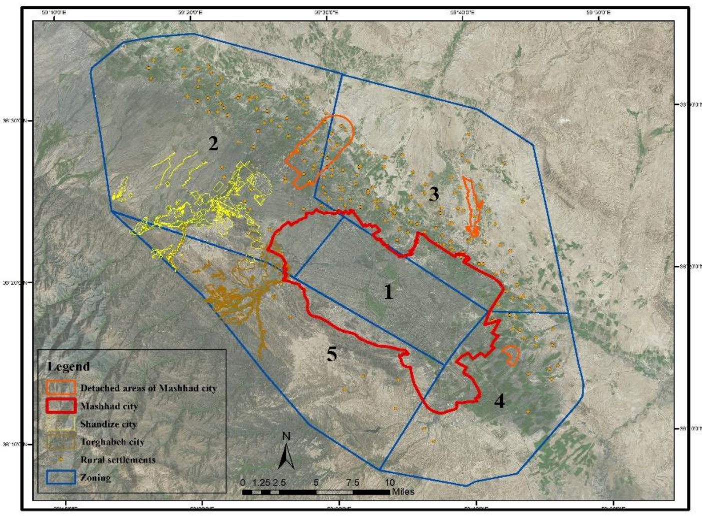

Fig. 3. Zoning of Mashhad Metropolitan area

Source: research findings based on metropolitan vector data

Table 2. Conditions of land cover changes from 2000 to 2010 and from 2010 to 2020

Zone	Rate of built-up development in 2000–2010	Rate of built-up development in 2010–2020	Priority of land-cover conversions
1	7.5%	9%	Barren to built-up
2	48.5%	34%	Barren to built-up
3	28	34%	Green space to built-up
4	13	19%	Barren to built-up Rock to built-up[1]
5	3	4%	Green space to built-up
Total	22%	30%	-

Source: research findings, 2023

[1]The conversion of rock land to built-up areas typically occurs through urbanization processes where natural land is excavated and developed to create infrastructure and residential and commercial spaces, driven by increasing population density and economic development. The construction of the southern road and the city's master plan programs have also influenced the process of transforming rock areas into built-up areas.

```
to develop_zone_2030 [zone cnt ]

 ;let total count patches with[not isNaN p_zone]
 ask up-to-n-of cnt patches with [p_zone = zone ][

   if zone = 1 and p_2020 = 4
   and count neighbors with [p_2020 = 1] > 0
   and general-condition?

   [set p_2030_p 1
     show-plot
     set pcolor item 0 lu-colors
     set dev_barren dev_barren + 1
   ]


   if (zone = 2 or zone = 3) and
   count neighbors with [p_2020 = 1] > 0
   and general-condition?
   [
     if  p_2020 = 4
     [set p_2030_p 1 set pcolor item 0 lu-colors set dev_barren dev_barren + 1]
     if  p_2020 = 3
     [ifelse count neighbors with [p_2020 = 4] > 0
       [ask one-of neighbors with [p_2020 = 4][set p_2030_p 1 set pcolor item 0 lu-colors set dev_barren dev_barren + 1 ]]
       [if not protected?  [set p_2030_p 1 set dev_veg dev_veg + 1 set pcolor item 0 lu-colors]]
     ]
```

Fig. 4. NetLogo Map set up
Source: research findings, 2023

it possible to explore the connection between the micro-level behavior of individuals and the macro-level patterns that emerge from their interaction (Wilensky, 1999).

2.3.1. Driving variables of LC

Since there is no general set of variables for LC, driving variables depend on the spatial LC changes in study areas.

According to the characteristics of the area and the findings of previous studies (Al Rifat & Liu 2022; Morshed et al. 2022; Mungai et al. 2022; Dietz et al. 2023), the following variables are selected: 1) built-up areas, 2) roads, 3) rocks, 4) green spaces, 5) barren lands, 6) water bodies, and 7) slopes.

2.3.2. LC changes the framework of the proposed model

In the absence of a developed LC simulation model, an ABM has been created and implemented as a prototype to model the LC mechanism in the context of the metropolitan area. This model grows land-cover patterns established in urban development plans, land topography and street networks. The model begins by representing the surface of a territory of MMA in 2020 (Fig. 5). Policymakers, developers and households are associated with distinct developer agents, which act in a simulated environment called the "world". The world consists of a rectangular grid of atomic areas called "patches", which store local attributes such as slope and five land-cover categories "built-up", "water bodies", "green spaces", "barren lands" and "rocks". The LC is coded according to categories. A patch is equivalent to a cell in a grid; each patch (cell) in this grid is interested in developing one of five possible land covers based on defined rules and conditions. We improved LC simulation by adding (1) rules to make structures for land-cover changes and (2) conditions responding to specific situations and urban policies on the system level. At each step (tick), some new points such as new built-up areas are interested in generating from built-up areas in one of the centroids of the metropolitan area. Indeed, agents evaluate the potential value of each neighboring cell according to the rules and conditions and adjacent roads (roads increase the potential value of neighboring cells).

If the potential value has specified rules and conditions, the cell becomes potentially developed. If not, the cell remains undeveloped. Therefore, users may steer the simulation by switching green spaces development slide limitations, which allow agents to develop green spaces or not. Finally, the model generates a rasterized map of land covers based on defined categories. This method led to evaluating the heterogeneous agents' interactions over time in a quantitative manner. It is designed for bottom-up analysis, the ABM captures a system's emergent behavior and accounts for system complexity (Derkenbaeva et al., 2023).

2.3.3. Possible scenarios of LC changes

The scenarios developed in this research are based on the defined conditions, allowing for an in-depth examination of how varying parameters can influence LC outcomes. By manipulating the conditions (Table 2) while keeping the rules constant (Table 1), we aim to derive insights into potential future LC changes. In the conditions table (Table 2), built-up rate growth in each zone is used as a certain built-up development threshold in planning scenarios. So, setting different thresholds for built-up land-cover development led to planning different scenarios, which allows one to evaluate the effects of urban policies.

Through this structured methodology, we ensure that our agent-based model remains scientifically rigorous and transparent, facilitating a clearer understanding of land-cover dynamics within the study area.

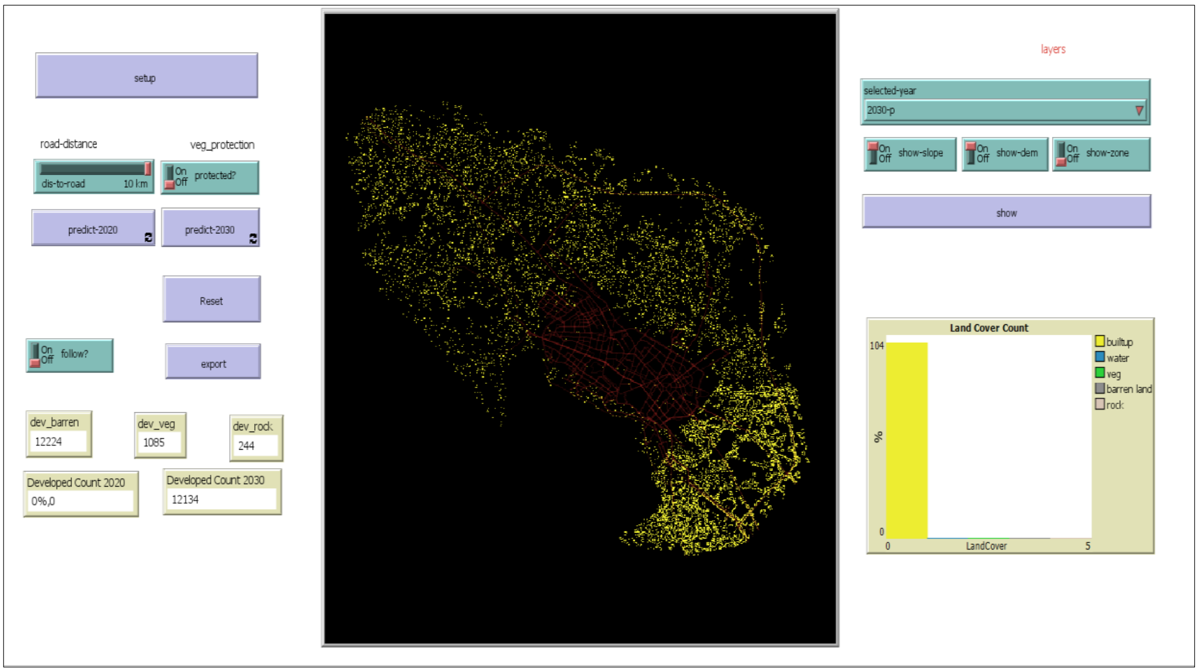

Fig. 5. Graphical interface and model output in NetLogo
Source: research findings, 2023

- **First scenario: continuation of the current trend**

To predict 2030 in the first scenario, it is assumed that the current trend will continue to 2030, Therefore, according to Table 2 conditions, the growth rate of the built-up category for each zone in 2030 will be equivalent to that in 2020 as a certain built-up development threshold. In this scenario, the cell search for development continues and tries to reach the threshold in each zone (Fig. 6). This means that a certain threshold may not be met exactly. Rather, they will be the base of the simulation, and the model will try to get as close to it as possible by considering other rules. Consequently, according to the defined rules (Table 1) and conditions (Table 2), the growth rate of the built-up category may be lower or higher than a certain threshold.

- **Second scenario: the environmental scenario**

In this scenario, as in the first one, a certain built-up development threshold is applied in each zone (Table 2). However, to preserve green spaces, with switching on the green space development restriction key, development in green areas will be limited. Green space will not be allowed to develop and convert to the built-up category.

- **Third scenario: free development**

In this scenario, there is no certain built-up development threshold. Indeed, there is no condition for built-up growth, and built-up patches (cells) can grow freely. Non-built-up patches can convert into built-up ones based on specified rules (Table 1), but without considering any specific threshold.

- **Fourth scenario: centrality of the Holy Shrine**

According to the idea proposed in the urban management of Mashhad city to direct the development towards the east of MMA to strengthen the geographical centrality of the Holy Shrine of Imam Reza (as the focal point of Mashhad tourism), in this scenario, built-up development threshold in each zone is set in such a way that the direction of the development moves to zone number 4 (double the previous one). In this scenario, the green space development restriction key is also off.

2.3.4. Model validation

With appropriate validation, the models can be evaluated on the prediction accuracy or their effectiveness. One common validation methodology for agent-based modeling is comparing the simulation results with the real-world data (Gong et al., 2023), which is also used by present scholars. To validate the LC simulation in the NetLogo platform by this method, simulation output data of land cover is compared with real data in 2020 according to the rules of Table 1 and the built-up growth rate of 2000–10 as conditions (Table 2). The differences between the simulated results and real-world observations can reliably evaluate the effectiveness of the proposed LC model. To evaluate the differences between the simulated results and real-world observations, the raster output of this simulation was exported to GIS software. The simulated output was converted into points to use the accuracy assessment points method to quantify the reliability of the simulated model. Indeed, the simulated land cover of these points is compared with real land cover in 2020. Afterward, the

```
to predict-2030

  develop_zone_2030 1 round (9 / 100 * get-total-valid-patches * .3)
  develop_zone_2030 2 round (34 / 100 * get-total-valid-patches * .3)
  develop_zone_2030 3 round (34 / 100 * get-total-valid-patches * .3)
  develop_zone_2030 4 round (19 / 100 * get-total-valid-patches * .3)
  develop_zone_2030 5 round (4 / 100 * get-total-valid-patches * .3)

   tick

end
```

Fig. 6. Setting conditions in first scenario
Source: research findings, 2023

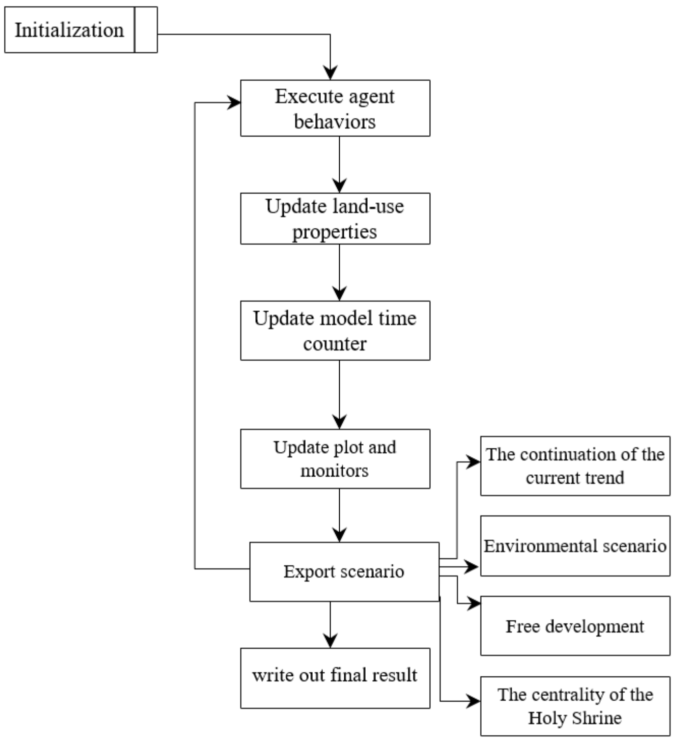

Fig. 7. NetLogo Flowchart

Table 3. Confusion matrix

–	Built-up areas' samples (x_{ii})	Other classes samples	Total number of samples (*N*)	Kappa
Built-up area	500	50	550	
Other class samples	70	620	690	0.794557
Total	570	670	1240	

number of correct and incorrect simulated points construct an error matrix in Excel to measure Cohen's kappa coefficient in Eq. 1 (Rahnama & Wyatt, 2021).

$$k = \frac{N\sum_{i=1}^{r} x_{ii} - \sum_{i=1}^{r}(x_{i+} * x_{+i})}{N^2 - \sum_{i=1}^{r}(x_{i+} * x_{+i})} \qquad (1)$$

Where *N* is the Total Number of Samples, *r* is the Number of Classes, x_{ii} represents Diagonal Values in the Matrix (395), x_{i+} could be considered as the Total Sample in Row I, and x_{+i} shows the Total Sample in column I.

In this simulation, Kappa is equal to 0.79. Therefore, the validity of the performed simulation has been evaluated as good (Fleiss et al., 2003). Therefore, the rules, conditions and codes could simulate LC changes in the MMA in a good manner.

Table 4. LC of MMA in 2000, 2010 & 2020

Year	2000		2010		2020		2000–2010	2010–2020	2000–2020
Land use	Area(ha)	percentage	Area(ha)	percentage	Area(ha)	percentage	Percent changes	Percent changes	Percent changes
Built-up	36,154	19.93	44,129	24.32	57,458	31.67	22.06	30.20	58.92
Water bodies	200	0.11	168	0.09	715	0.39	-16.20	326.32	257.26
Green spaces	45,593	25.13	38,876	21.43	38,364	21.15	-14.73	-1.32	-15.86
Barren lands	61,886	34.11	59,945	33.04	45,963	25.34	-3.14	-23.32	-25.73
Rocks	37,586	20.72	38,302	21.11	38,920	21.45	1.91	1.61	3.56
Total	181,419	100.00	181,419	100.00	181,419	100.00	-	-	_

Source: research findings, 2023

3. Research results

3.1. LC analysis (2000–2020)

The analysis of LC changes in the MMA between 2000 and 2010 indicates that, while rock formations remained relatively stable, built-up areas experienced the most significant transformation, with an increase of over 22% during this decade. In addition to built-up areas, water bodies and barren lands also underwent considerable changes; specifically, water bodies decreased by more than 16%, and green spaces declined by over 14%. Additionally, built-up areas expanded by 30%, contrasted with a reduction of more than 23% in barren lands during the same period. The most pronounced changes were observed in the western part of MMA from 2000 to 2010. In the subsequent period from 2010 to 2020, the most significant changes occurred primarily in the northern and western regions of the MMA. Table 4 presents the LC classifications for the MMA from 2000 to 2020.

3.2. LC analysis (2020–2030)

To write different scenarios for the development of the MMA, different possible scenarios have been implemented several times. It is obvious that different pixels are randomly developed in each execution and subsequently the developed areas will also be different. But to register the developed model, the most repeated mode is considered. In Table 5, the number of pixels developed in each scenario is written.

Table 5 indicates the level of development achieved by each of the five zones (Fig. 3).

3.2.1. First scenario: continuation of the current trend

According to Table 6, the developed areas (transformation of other areas to built-up areas) in this scenario are about 5,920 hectares. Even though the development rate in Zone 4 is more than other zones (0.21), Zones 3 and 2 are the most

Table 5. Number of pixels developed in different scenarios

scenarios	First scenario: continuation of the current trend		Second scenario: the environmental scenario		Third scenario: free development		Fourth scenario: centrality of the Holy Shrine	
Land use	Developed pixels		Developed pixels		Developed pixels		Developed pixels	
	Area(ha)	percentage	Area(ha)	percentage	Area(ha)	Percentage	Area(ha)	percentage
Barren lands	2,306.77	38.96	2,302.11	78.08	5,508.25	34.93	1,994.91	30.01
Green spaces	2,905.60	49.08	0.00	0.00	7,150.04	45.35	3,139.91	47.24
Rocks	708.24	11.96	646.46	21.92	3,110.66	19.72	1,512.53	22.75
Total	5,920.61	100.00	2,948.57	100.00	15,768.96	100.00	6,647.36	100.00

Source: research findings, 2023

developed parts of MMA. Green spaces are the most developed classes compared to other classes. Due to the presence of agricultural lands in Zone 3, the green spaces have been significantly damaged by the development of Mashhad in the first scenario.

In Zone 2, there are two main development centers: Shandiz City and Mashhad–Cheneran Road. Development radiates outwards from these centers. The western area of Mashhad has experienced minimal development, with the primary focus remaining around Mashhad–Chenaran Road (Fig. 8). Satellite image analysis from 2000 to 2020 underscores the pivotal role of this axis in the west's development, making it a key focal point for the region's growth. Consequently, the development of MMA in the western part is discrete development, and Mashhad–Chenaran Road emerges as the most crucial center of development. The conversion of green spaces into built-up areas is clear in this scenario.

In the eastern part of Mashhad, the main road (Mashhad–Neishabour), play a critical role in the development of the eastern region (Fig. 8).

3.2.2. Second scenario: the environmental scenario

Due to constraints on developing green spaces in the second scenario, the amount of developed land has been reduced by half compared to the previous scenario, (decreasing from ~6,000 to ~3,000). Barren lands are converted into built-up areas, while green spaces remain unchanged. According to Table 6 and Fig. 8, Zone 2 exhibits the strongest inclination for development, and the development rate in Zone 4 is more than other zones (0.09). The development of Zone 3 has been approached separately to ensure the preservation of green spaces. Furthermore, the development of Zone 2

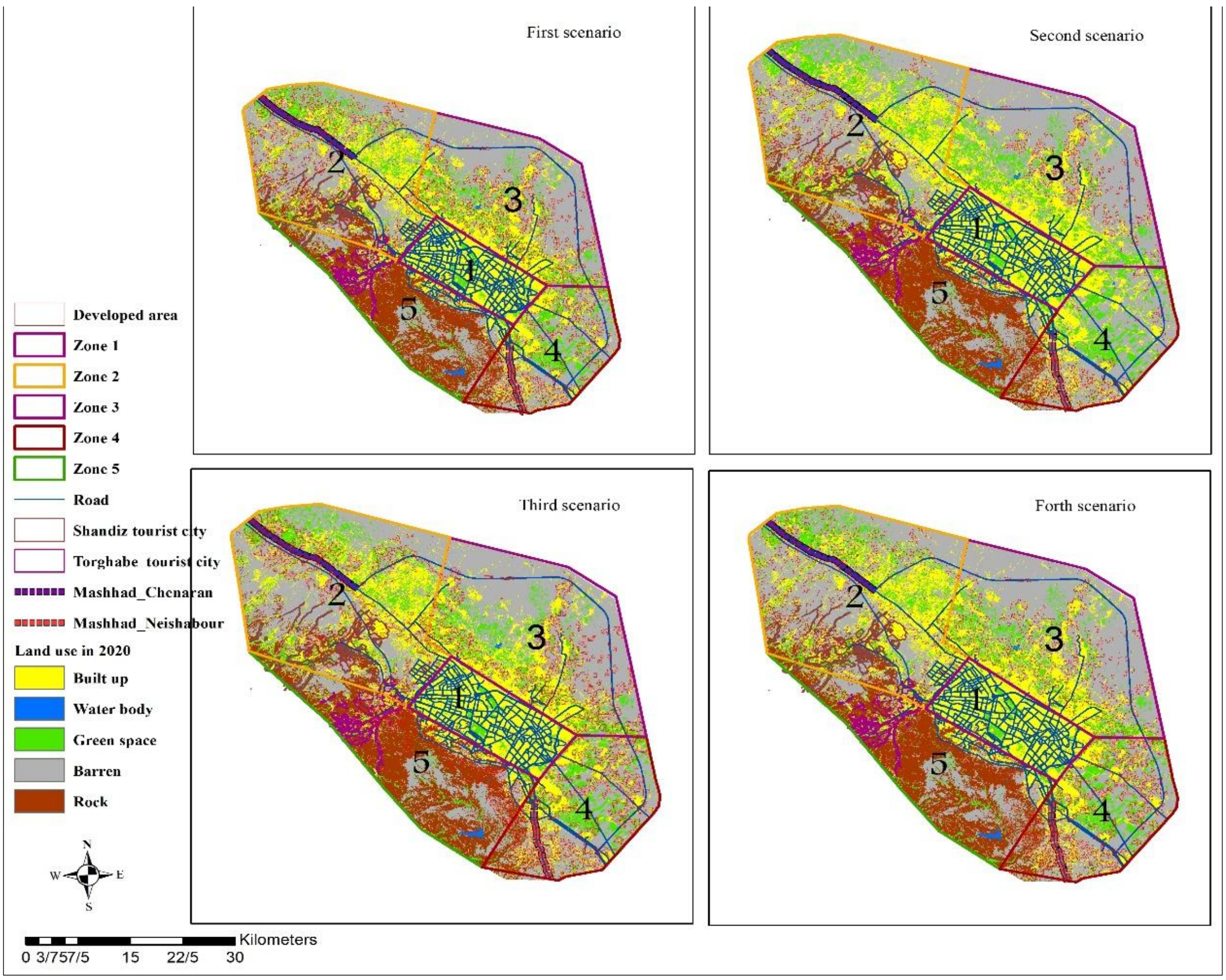

Fig. 8. LULC scenarios in Mashhad Metropolitan area
Source: research findings, 2023

Table 6. Amount of development of each zone in different scenarios

		First scenario: continuation of the current trend				Second scenario: the environmental scenario				Third scenario: free development				Fourth scenario: centrality of the Holy Shrine			
	Built-up area in 2020	Developed area		Built-up area in 2030	Growth rate	Developed area		Built-up area in 2030	Growth rate	Developed area		Built-up area in 2030	Growth rate	Developed area		Built-up area in 2030	Growth rate
zone	hectares	hectares	Percent	hectares	percent	hectares	percent	hectares	percent	hectares	percent	hectares	percent	hectares	percent	hectares	percent
1	14420.8	0.79	0.01	14421.59	0	0	0	14420.8	0	0	0	14420.80	0	1	0.02	14421.80	0
2	18595.9	2103.9	35.54	20699.8	0.11	1145.89	38.86	19741.79	0.06	4820.35	30.57	23416.25	0.25	1367.5	20.57	19963.40	0.07
3	12085.2	2239.2	37.82	14324.45	0.19	1019.71	34.58	13104.91	0.08	4655.98	29.53	16741.18	0.38	1447.17	21.77	13532.37	0.12
4	6955.2	1445.9	24.42	8401.1	0.21	662.53	22.47	7617.73	0.09	4616.47	29.28	11571.67	0.66	3505.74	52.74	10460.94	0.50
5	4241.4	130.79	2.21	4372.19	0.13	120.46	4.09	4361.86	0.02	1676.16	10.63	5917.56	0.39	325.95	4.90	4567.35	0.08
Total	56298.5	5920.6	100	62219.13	0.11	2948.59	100	59247.09	0.05	15768.96	100	72067.46	0.28	6647.36	100	62945.86	0.12

Source: research findings, 2023

along the Mashhad–Chenaran Road is restricted to the southern side of the road. Furthermore, in this scenario, the Mashhad–Neishabour Road in the southeast of Mashhad serves as another key axis for development (Fig. 8).

3.2.3. Third scenario: free development

Since in the third scenario, the development has been conducted freely, the area of developed lands is much larger than in other scenarios. The developed areas (transformation from other areas to built-up) in this scenario are about 15,769 hectares. Based on Table 5 and Fig. 8, Zone 2 experiences the highest level of development, while Zones 3 and 4 exhibit similar levels of development. The development rate in Zone 4 is more than other zones (0.66). In the third scenario, roads play a more important role in developing the surroundings process. Development in this scenario is characterized by a more concentrated, cohesive and continuous pattern compared to the previous scenarios. Additionally, Torghabe City, along with Shandiz, is recognized as a key center for development. The southern region of Mashhad City experiences heightened development, with more mountainous areas being developed. The physical expansion towards the southern heights of the city has intensified under the influence of the preparation of comprehensive urban plans and the construction of the southern highway (Fig. 8).

3.2.4. Fourth scenario: centrality of the Holy Shrine

By Table 6 and Fig. 8, in the fourth scenario, after Zone 4, which has developed more than 50%, Zones 2 and 3 have developed to the same extent. The developed areas are about 6,647 hectares and the development rate in Zone 4 is more than other zones (0.50). The development of the east has been centered on the main roads, especially the Mashhad–Neishabour Road, but Zone 3 has been developed in a more scattered way.

4. Discussion

Over the past 20 years (2000–20), the MMA has experienced rapid economic and political-administrative concentration, the emergence of religious-tourism centers, increased industrial activities and significant rural–urban migration. These factors have led to notable changes in LULC. This paper analyzes the LC changes within the MMA, which encompasses an area of 181,419 hectares. In this regard, the present research is conducted in two parts. The first part addresses the classification of LC in MMA using the SVM algorithm, examining changes from 2000 to 2020 in five zones. In this section, some rules and conditions are extracted from LC analysis.

The analysis of LC changes from 2000 to 2010 highlights significant growth in built-up areas, with an increase of over 22%. This growth mainly occurred on green spaces and barren lands, in the western part of MMA (Zone 2). From 2010 to 2020, there was a shift in the development of built-up areas towards both the north and west of the area (Zones 2 and 3). However, due to the presence of informal settlements in the northern region (Zone 3), the changes observed indicate that informal settlements experienced more development from 2010 to 2020 compared to the previous decade.

The second part simulates these changes for the year 2030 based on the extracted rules and conditions, utilizing ABM in NetLogo software. The variables studied in this research are 1) built-up areas, 2) roads, 3) rocks, 4) green spaces, 5) barren lands, 6) water bodies and 7) slope.

The research modeling for 2030 indicates that the direction of the city's development is towards the north (Zone 3) and west (Zone 2). According to the analysis provided, it is evident that the development of Zone 2 is a key focus in two scenarios, in that, the growth rate of built-up land cover is more than 30%. In this zone, built-up areas will be developed through the barren lands. The existence of the Mashhad–Chenaran Road as the key axis of development is considered the source of concentration and density of development in this zone. Due to the city's development plans, the west side of MMA is earmarked for future development. However, the actual development of Zone 2 is anticipated to occur in an unplanned area, specifically around the Mashhad–Chenaran Road, resulting in the formation of informal settlements. This unexpected shift highlights the challenges of urban planning and the complexities of managing urban growth, underscoring the need for strategic interventions to address the evolving urban landscape and ensure sustainable development in the region.

The development of Zone 3 involves a transition in land cover in such a way that the green spaces in the northern part of the area will be converted into built-up. Built-up areas will also be developed through the barren lands. These transitions particularly occurred in unplanned areas characterized by informal settlements.

Overall, the evaluation of the research scenarios indicates that the northern part of MMA may be at risk of extensive marginalization, while the south-west region, particularly Shandiz, is poised for tourism-driven growth. Moreover, the focus on centralizing the holy shrine has implications for heightened development in the eastern region, presenting both new opportunities and risks compared to previous decades.

The expansion toward the east also appears to have fostered two divergent patterns within the city: the westward movement of upper-middle-class populations and the eastward growth of lower-middle-class residents. This shift has been accompanied by unplanned expansion and increased marginalization in the eastern areas, leading to potential crises in green spaces, a developmental rift within the metropolitan framework, and a significant decline in the sustainability of the region's urban systems. Such findings highlight the intricate interactions within the study area, calling for careful consideration and strategic planning in sustainable land management.

The modeling results show that population growth and unplanned urbanization have impacted the functions of ecosystems and accounted for this loss. These findings are consistent with those of Rahnama and Wyatt (2021) in Melbourne, Morshed et al. (2022) in Jashore City, Bangladesh, Zhao et al. (2022) in Shenzhen City, Mahmoudzadeh and Naghdbishi (2021) in Neyshabur, and Han et al. (2015) in Beijing, revealing that rapid growth in built-up areas results in a continuous decrease in green spaces. The spatial growth of the urban area toward the surrounding suburbs, especially in the west and north of Mashhad, aligns to a large extent with the forecasts of Dadashpoor and Jahanzad (2016) and Rahnamaa (2021) predicting that urban development could impact Mashhad's natural environment. Notably, main roads such as Mashhad–Chenaran, Mashhad–Nishabour, and urban centers like Torghaba and Shandiz cities play pivotal roles as development hubs in the current study. These evidences show that developers, especially business owners, may prefer to invest near other investors and main roads. These conclusions have also been confirmed in business location-allocation studies (Mohammed, 2023; Kimelberg & Williams, 2013; Bartik, 2012).

NetLogo, a multi-agent modeling environment, has seen limited application in urban studies. Zhaka and Xhina (2021) used the NetLogo GIS Extension to visualize geospatial data for Canada's provinces, aiming to support future agent-based urban models, but lacking substantial modeling. Chicaiza Ortiz et al. (2022) examined urban interventions in Tena, Ecuador, also using NetLogo, but their model did not consider land use, neglected uncertainties, and focused on a single scenario. In contrast, Batty (1998) employed an extended cellular automaton framework to analyze spontaneous urban growth in a hypothetical context, while Berr (1998) used a grid format without accounting for urbanization or various scenarios, limiting real-world applicability.

This research differentiates itself from prior studies using NetLogo in two significant ways:

1. **Scenario Diversity:** It offers multiple scenarios, accounting for past trends and potential policy changes, thereby addressing uncertainties and enhancing model flexibility. Other studies typically focus on a single, definitive future without exploring various development options.
2. **Contextual Authenticity:** The modeling is grounded in an actual territory rather than hypothetical environments, increasing its relevance for urban planning by reflecting real-world constraints of existing land covers.

To illustrate this approach, an interactive scenario modeling tool has been developed using MMA data. For broader applicability, two steps are essential: creating land-cover, road-network and topographical maps for the district to serve as inputs for the NetLogo tool, and tailoring the rules and conditions to reflect local status and policies. This systematic approach ensures that the model remains adaptable for various urban contexts.

5. Conclusions

This study analyzed LC changes in MMA, covering 181,419 hectares, by utilizing Landsat 7 and 8 imagery in two parts: the first part focuses on examining LC changes from 2000 to 2020, while the second part simulates these changes for 2030. In the first part, the SVM algorithm was employed to analyze shifts in LC categories during 2000 to 2020. The findings reveal a substantial increase in built-up areas, expanding by 21,303 hectares (58.92%), alongside notable reductions in barren lands and green spaces, which decreased by 15,922 hectares (25.73%) and 7,229 hectares (15.86%), respectively. Furthermore, we conducted spatial simulations to project LC changes for 2030 using ABM in NetLogo, exploring four distinct scenarios: 1) Continuation of the current trend, 2) The environmental scenario, 3) Free development, and 4) Centrality of the Holy Shrine. The results indicate that Mashhad city is expanding predominantly toward the north and west, with informal settlements increasingly encroaching upon green spaces. Additionally, enhanced road access is anticipated to accelerate urban land expansion further. The projected LC map for 2020 was validated against the actual map using the Kappa coefficient (0.7945), demonstrating a high level of accuracy for the model.

The proposed model provides valuable empirical evidence regarding the impact of urban policies on LC changes, suggesting that city officials can use these research-informed simulation results to enhance decision-making processes. To build upon this study, future research should explore additional factors influencing LULC changes and the broader urban development process. Furthermore, refining the simulation model to differentiate among various types and behaviors of developers will help identify which developers exert the most significant influence on urban transitions.

References

Abar, S., Theodoropoulos, G.K., Lemarinier, P., & O'Hare, G. M. (2017). Agent Based Modelling and Simulation tools: A review of the state-of-art software. *Computer Science Review*, *24*: 13-33. DOI: https://doi.org/10.1016/j.cosrev.2017.03.001.

Achter, S., Borit, M., Cottineau, C., Meyer, M., Polhill, J.G., & Radchuk, V. (2024). How to conduct more systematic reviews of agent-based models and foster theory development-Taking stock and looking ahead. *Environmental Modelling & Software, 173*: 105867. DOI: https://doi.org/10.1016/j.envsoft.2023.105867.

Angel, S., Parent, J., Civco, D. L., Blei, A., & Potere, D. (2011). The dimensions of global urban expansion: Estimates and projections for all countries, 2000–2050. *Progress in Planning*, *75*(2): 53-107. DOI: https://doi.org/10.1016/j.progress.2011.04.001.

Arabi Aliabad, F., Shojaei, S., Zare, M., & Ekhtesasi, M.R. (2019). Assessment of the fuzzy ARTMAP neural network method performance in geological mapping using satellite images and Boolean logic. *International journal of environmental science and technology*, *16*: 3829-3838. DOI: https://doi.org/10.1007/s13762-018-1795-7.

Bartik, T.J. (2012). Including jobs in benefit-cost analysis. *Annual Review of Resource Economics*, *4*(1): 55-73. DOI: https://doi.org/10.1146/annurev-resource-110811-114520.

Batty, M. (1998). Urban evolution on the desktop: simulation with the use of extended cellular automata. *Environment and planning A*, *30*(11): 1943-1967. DOI: https://doi.org/10.1068/a301.

Beerman, J.T., Beaumont, G.G., & Giabbanelli, P.J. (2023). A framework for the comparison of errors in agent-based models using machine learning. *Journal of computational science, 72:* 102119. DOI: https://doi.org/10.1016/j.jocs.2023.102119.

Cao, Z., Zhu, J., Tang, B., & Chen, T. (2023). System dynamics simulation of occupational health and safety management causal model based on NetLogo. *Heliyon, 9*(8). DOI: https://doi.org/10.1016/j.heliyon.2023.e18752.

Chachondhia, P., Shakya, A., & Kumar, G. (2021). Performance evaluation of machine learning algorithms using optical and microwave data for LULC classification. *Remote Sensing Applications: Society and Environment, 23*: 100599. DOI: https://doi.org/10.1016/j.rsase.2021.100599.

Chen, D., Ma, A., & Zhong, Y. (2023). Semi-supervised knowledge distillation framework for global-scale urban man-made object remote sensing mapping. *International Journal of Applied Earth Observation and Geoinformation, 122:* 103439. DOI: https://doi.org/10.1016/j.jag.2023.103439.

Coronese, M., Occelli, M., Lamperti, F., & Roventini, A. (2023). AgriLOVE: agriculture, land-use and technical change in an evolutionary, agent-based model. *Ecological Economics, 208:* 107756. DOI: https://doi.org/10.1016/j.ecolecon.2023.107756.

Daams, M.N., Banquet, A., Delbouve, P., & Veneri, P. (2023). Consistent metropolitan boundaries for the remote sensing of urban land. *Remote Sensing of Environment, 297:* 113789. DOI: https://doi.org/10.1016/j.rse.2023.113789.

Dadashpoor, H., Jahanzad, N., & Jalili, H. (2016). Analysis and forecasting of the integrated spatial structure in Mashhad metropolitan region in the period 1996-2041. *Motaleate Shahri*, *5*(18): 51-62.

Darrel Jenerette, G., & Potere, D. (2010). Global analysis and simulation of land-use change associated with urbanization. *Landscape ecology, 25:* 657-670.

Derkenbaeva, E., Hofstede, G.J., van Leeuwen, E., & Vega, S.H. (2023). Simulating households' energy transition in Amsterdam: An agent-based modeling approach. *Energy Conversion and Management, 294:* 117566. DOI: https://doi.org/10.1016/j.enconman.2023.117566.

De Souza Silva, I., Nascimento, D.T.F., de Araújo Romão, P., da Silva, G.D.F.N., Sales, M.M., & da Luz, M.P. (2023). Proposition of LULC mapping in progressive detailing for the surroundings of hydroelectric powerplant reservoirs: Case study for the Batalha (Brazil). *International Journal of Applied Earth Observation and Geoinformation, 118:* 103218. DOI: https://doi.org/10.1016/j.jag.2023.103218.

De Visscher, L., De Baets, B., & Baetens, J. M. (2023). A critical review of common pitfalls and guidelines to effectively infer parameters of agent-based models using Approximate Bayesian Computation. *Environmental Modelling & Software*, 105905. DOI: https://doi.org/10.1016/j.envsoft.2023.105905.

Dicks, M., Paskaramoorthy, A., & Gebbie, T. (2024). A simple learning agent interacting with an agent-based market model. *Physica A: Statistical Mechanics and its Applications*, *633*: 129363. DOI: https://doi.org/10.1016/j.physa.2023.129363.

Dixon, B., & Candade, N. (2008) Multispectral landuse classification using neural networks and support vector machines: one or the other, or both? *International Journal of Remote Sensing, 29*(4): 1185-1206. DOI: https://doi.org/10.1080/01431160701294661.

Fleiss, J.L., Levin, B., & Paik, M.C. (2013). *Statistical methods for rates and proportions*. John Wiley & Sons.

Fu, X., Wang, X., & Yang, Y. J. (2018). Deriving suitability factors for CA-Markov land use simulation model based on local historical data. *Journal of environmental management, 206:* 10-19. DOI: https://doi.org/10.1016/j.jenvman.2017.10.012.

General population and housing censuses of Iran. (2016). Iran's official statistics website. Available at: https://amar.org.ir.

Gomes, E., Banos, A., Abrantes, P., Rocha, J., & Schläpfer, M. (2020). Future land use changes in a peri-urban context: Local stakeholder views. *Science of the total environment*, *718*: 137381. DOI: https://doi.org/10.1016/j.scitotenv.2020.137381.

Gong, S., Dong, X., Wang, K., Lei, B., Jia, Z., Qin, J., & Cao, R. (2023). Agent-based modelling with geographically weighted calibration for intra-urban activities simulation using taxi GPS trajectories. *International Journal of Applied Earth Observation and Geoinformation, 122:* 103368. DOI: https://doi.org/10.1016/j.jag.2023.103368.

Han, H., Yang, C., & Song, J. (2015). Scenario simulation and the prediction of land use and land cover change in Beijing, China. *Sustainability, 7*(4): 4260-4279. DOI: https://doi.org/10.3390/su7044260.

Huang, D., Huang, J., & Liu, T. (2019). Delimiting urban growth boundaries using the CLUE-S model with village administrative boundaries. *Land use policy, 82:* 422-435. DOI: https://doi.org/10.1016/j.landusepol.2018.12.028.

Huang, Y., Li, L., & Yu, Y. (2018). Does urban cluster promote the increase of urban eco-efficiency? Evidence from Chinese cities. *Journal of Cleaner Production*, *197*: 957-971. DOI: https://doi.org/10.1016/j.jclepro.2018.06.251.

Innocenti, E., Detotto, C., Idda, C., & Prunetti, D. (2019). Urban, agricultural and touristic land use patterns: combining spatial econometrics and ABM/LUCC. In *2019 4th World Conference on Complex Systems (WCCS)*. IEEE. DOI: 10.1109/ICoCS.2019.8930776.

Irwin, E.G., & Geoghegan, J. (2001). Theory, data, methods: developing spatially explicit economic models of land use change. *Agriculture, Ecosystems & Environment, 85*(1-3): 7-24. DOI: https://doi.org/10.1016/S0167-8809(01)00200-6.

Islam, M.R., & Esraz-Ul-Zannat, M. (2023). Remote sensing-based investigation of coastal LULC dynamics in the coastal region of Bangladesh. *Remote Sensing Applications: Society and Environment, 31:* 100982. DOI: https://doi.org/10.1016/j.rsase.2023.100982.

Jasim, B.S., Jasim, O.Z., & AL-Hameedawi, A.N. (2024). Evaluating land use land cover classification based on machine learning algorithms. *Engineering and Technology Journal*, *42*(5): 557-568. DOI: https://doi.org/10.30684/etj.2024.144585.1638.

Jijo, B.T., & Abdulazeez, A. M. (2021). Classification based on decision tree algorithm for machine learning. *evaluation, 6:* 7. DOI: https://doi.org/10.38094/jastt20165.

Kafy, A.A., Shuvo, R.M., Naim, M.N.H., Sikdar, M.S., Chowdhury, R.R., Islam, M.A., & Kona, M.A. (2021). Remote sensing approach to simulate the land use/land cover and seasonal land surface temperature change using machine learning algorithms in a fastest-growing megacity of Bangladesh. Remote Sensing Applications: *Society and Environment, 21:* 100463. DOI: https://doi.org/10.1016/j.rsase.2020.100463.

Kamran, M., Khokhar, M.F., Waheed, A., Khan, J.A., & Khayyam, U. (2022). Exploring the Nexus between Land Use Land Cover (LULC) Changes and Population Growth in Planned and Unplanned Cities. *Available at SSRN 4261709*. DOI: https://doi.org/10.1016/j.heliyon.2023.e13297.

Kamusoko, C., Aniya, M., Adi, B., & Manjoro, M. (2009). Rural sustainability under threat in Zimbabwe–simulation of future land use/ cover changes in the Bindura district based on the Markov-cellular automata model. *Applied Geography, 29*(3): 435-447. DOI: https://doi.org/10.1016/j.apgeog.2008.10.002.

Karali, E., Rounsevell, M.D., & Doherty, R. (2011). Integrating the diversity of farmers' decisions into studies of rural land-use change. *Procedia Environmental Sciences, 6*: 136-145.

Kimelberg, S.M., & Williams, E. (2013). Evaluating the importance of business location factors: The influence of facility type. *Growth and Change, 44*(1): 92-117. DOI: https://doi.org/10.1111/grow.12003.

Koomen, E., & Buurman, J.J.G. (2002). Economic theory and land prices in land use modeling. In *Papers of 5th AGILE conference on Geographic Information Science*.

Kucsicsa, G., Popovici, E.A., Bălteanu, D., Grigorescu, I., Dumitraşcu, M., & Mitrică, B. (2019). Future land use/cover changes in Romania: regional simulations based on CLUE-S model and CORINE land cover database. *Landscape and ecological engineering, 15*(1): 75-90. DOI: https://doi.org/10.1007/s11355-018-0362-1.

Lai, Y. (2023). Optimization of urban and rural ecological spatial planning based on deep learning under the concept of sustainable development. *Results in Engineering, 19:* 101343. DOI: https://doi.org/10.1016/j.rineng.2023.101343.

Lang, D., & Ertsen, M.W. (2023). Modelling farmland dynamics in response to farmer decisions using an advanced irrigation-related agent-based model. *Ecological Modelling, 486*: 110535. DOI: https://doi.org/10.1016/j.ecolmodel.2023.110535.

Lee, I.P.A., Eldakar, O.T., Gogarten, J.P., & Andam, C.P. (2023). Protocol for an agent-based model of recombination in bacteria playing a public goods game. *STAR protocols, 4*(4): 102733. DOI: https://doi.org/10.1016/j.xpro.2023.102733.

Li, F., Xie, Z., Clarke, K.C., Li, M., Chen, H., Liang, J., & Chen, Z. (2019). An agent-based procedure with an embedded agent learning model for residential land growth simulation: The case study of Nanjing, China. *Cities, 88*: 155-165. DOI: https://doi.org/10.1016/j.cities.2018.10.008.

Li, F., Yigitcanlar, T., Nepal, M., Nguyen, K., & Dur, F. (2023). Machine learning and remote sensing integration for leveraging urban sustainability: A review and framework. *Sustainable Cities and Society*, 104653. DOI: https://doi.org/10.1016/j.scs.2023.104653.

Li, Y., Cai, Y., Fu, Q., Zhang, X., Wan, H., & Yang, Z. (2024). Dynamics of Land Use/Land Cover Considering Ecosystem Services for a Dense-Population Watershed Based on a Hybrid Dual-Subject Agent and Cellular Automaton Modeling Approach. *Engineering*, 37: 182-195. DOI: https://doi.org/10.1016/j.eng.2023.10.015.

Liang, X., Liu, X., Li, D., Zhao, H., & Chen, G. (2018). Urban growth simulation by incorporating planning policies into a CA-based future land-use simulation model. *International Journal of Geographical Information Science, 32*(11): 2294-2316. DOI: https://doi.org/10.1080/13658816.2018.1502441.

Liu, D., Zheng, X., & Wang, H. (2020). Land-use Simulation and Decision-Support system (LandSDS): Seamlessly integrating system dynamics, agent-based model, and cellular automata. *Ecological Modelling, 417*: 108924. DOI: https://doi.org/10.1016/j.ecolmodel.2019.108924.

Mahmoodzadeh, H., & Naghdbishi, A. (2021). Comparative study of the efficiency of the urban development Agent based model and Markov chain Cellular Automata model for urban development simulation in the Neyshabur. *Geography and Development*, *19*(64): 291-314. DOI: 10.22111/J10.22111.2021.6352.

Mashhad Municipality. (2020). *Statistics of Mashhad, 2020*, Assistance of Planning and Human Capital Development of Mashhad Municipality under the supervision ofStatistics Management, Mashhad: Mashhad Municipality.

Marini, N., Otálora, S., Müller, H., & Atzori, M. (2021). Semi-supervised training of deep convolutional neural networks with heterogeneous data and few local annotations: An experiment on prostate histopathology image classification. *Medical image analysis, 73:* 102165. DOI: https://doi.org/10.1016/j.media.2021.102165.

Mohammed, A.M., & Ukai, T. (2023). Agent-based modelling for spatiotemporal patterns of urban land expansion around university campuses. *Modeling Earth Systems and Environment*, *9*(1): 1119-1133.

Morshed, S.R., Fattah, M.A., Haque, M.N., & Morshed, S.Y. (2022) Future ecosystem service value modelling with land cover dynamics by using machine learning based Artificial Neural Network model for Jashore city, Bangladesh. *Physics and Chemistry of the Earth, Parts a/b/c, 126*: 103021. DOI: https://doi.org/10.1016/j.pce.2021.103021.

Motieyan, H., & Mesgari, M.S. (2018). An agent-based modeling approach for sustainable urban planning from land use and public transit perspectives. *Cities, 81:* 91-100. DOI: https://doi.org/10.1016/j.cities.2018.03.018.

Motlaq, M.A., & Abbaszadeh, G. (2012). The physical development of Mashhad city and its environmental impacts. *Environment and Urbanization ASIA, 3*(1): 79-91. DOI: https://doi.org/10.1177/097542531200300105.

Mungai, L.M., Messina, J.P., Zulu, L.C., & Snapp, S. (2022) Modelling Spatiotemporal Patterns of Land Use/Land Cover Change in Central Malawi Using a Neural Network Model. *Remote Sensing*, *14*(14): 3477. DOI: https://doi.org/10.3390/rs14143477.

Nehzak, H.K., Aghaei, M., Mostafazadeh, R., & Rabiei-Dastjerdi, H. (2022). Assessment of machine learning algorithms in land use classification. In *Computers in Earth and Environmental Sciences*. Elsevier. DOI: https://doi.org/10.1016/B978-0-323-89861-4.00022-1.

Nganro, S., Trisutomo, S., Barkey, R., Ali, M., Imura, H., Onishi, A., Tsai, P.-I., & Mahamud, M.A. (2021). Prediction of Future Land Use and Land Cover (LULC) in Makassar City. *Tataloka*, *23*(2): 183-189.

Njoku, E.A., & Tenenbaum, D.E. (2022). Quantitative assessment of the relationship between land use/land cover (LULC), topographic elevation and land surface temperature (LST) in Ilorin, Nigeria. *Remote Sensing Applications: Society and Environment, 27:* 100780. DOI: https://doi.org/10.1016/j.rsase.2022.100780.

Nucci, L., Rahnama, M.R., & Heydari, A. (2016). Analysis the Process and Priorities of Urbanization in the Mashhad city After Islamic Revolution of Iran. *International journal, 2*(4). Available at: http://www.ijhcs.com/index.php/ijhcs/index.

Ortiz, A.F.C., Rodas, K.A.C., Pineda, A.P.C., Sandoval, J., Amaguaya, D.J.V., Gallo, A.D.V., Rosero, O.D.M., & Bustamante, A.F.M. (2022). Simulador para recrear las dinámicas urbanas de Tena con Netlogo, antes de la intervención del espacio público (Simulator to recreate the urban dynamics of Tena with Netlogo, before the intervention of the public space – in Spanish). *Eídos*, *14*(20): 39-44. DOI: https://doi.org/10.29019/eidos.v14i20.1005.

Ouma, Y., Nkwae, B., Moalafhi, D., Odirile, P., Parida, B., Anderson, G., & Qi, J. (2022). Comparison of machine learning classifiers for multitemporal and multisensor mapping of urban LULC features. The International Archives of the Photogrammetry, *Remote Sensing and Spatial Information Sciences, 43:* 681-689. DOI: https://doi.org/10.5194/isprs-archives-XLIII-B3-2022-681-2022.

Park, K. (2023). Regreening suburbia: An analysis of urban greening approaches in US sprawl retrofitting projects. *Urban Forestry & Urban Greening, 88:* 128092. DOI: https://doi.org/10.1016/j.ufug.2023.128092.

Pham, T.D., Xia, J., Ha, N.T., Bui, D.T., Le, N.N., & Takeuchi, W. (2019). A review of remote sensing approaches for monitoring blue carbon ecosystems: Mangroves, seagrasses, and salt marshes during 2010–2018. *Sensors, 19*(8): 1933. DOI: https://doi.org/10.3390/s19081933.

Potić, I., & Potić, M. (2017). Remote sensing machine learning algorithms in environmental stress detection-case study of Pan-European south section of corridor ten in Serbia. *Bulletin of Natural Sciences Research, 7*(2). DOI: https://doi.org/10.5937/univtho7-14957.

Qiu, R., Xu, W., Zhang, J., & Staenz, K. (2018). Modelling and simulating urban residential land development in Jiading New City, Shanghai. *Applied Spatial Analysis and Policy, 11:* 753-777.

Rahnama, M. R. (2021a). Forecasting land-use changes in Mashhad Metropolitan area using Cellular Automata and Markov chain model for 2016-2030. *Sustainable Cities and Society, 64*: 102548. DOI: https://doi.org/10.1016/j.scs.2020.102548.

Rahnama, M. R. (2021b). Simulation of land use land cover change in Melbourne metropolitan area from 2014 to 2030: Using multilayer perceptron neural networks and Markov chain model. *Australian Planner, 57*(1): 36-49. DOI: https://doi.org/10.1080/07293682.2021.1920994.

Rahnama, M.R., & Wyatt, R. (2021). Projecting Land use change with neural network and GIS in northern Melbourne for 2014–2050. *Australian Geographer, 52*(2): 149-170. DOI: https://doi.org/10.1080/00049182.2021.1920088.

Razaque, A., Ben Haj Frej, M., Almi'ani, M., Alotaibi, M., & Alotaibi, B. (2021). Improved support vector machine enabled radial basis function and linear variants for remote sensing image classification. *Sensors*, *21*(13): 4431. DOI: https://doi.org/10.3390/s21134431.

Ritu, S.M., Sarkar, S.K., & Zonaed, H. (2023). Prediction of Padma riverbank shifting and its consequences on LULC changes. *Ecological Indicators, 156*: 111104. DOI: https://doi.org/10.1016/j.ecolind.2023.111104.

Salem, M.B., Ettabaa, K.S., & Bouhlel, M.S. (2018). An unsupervised classification approach for hyperspectral images based adaptive spatial and spectral neighborhood selection and graph clustering. *Procedia Computer Science, 126*: 743-750. DOI: https://doi.org/10.1016/j.procs.2018.08.008.

Santarsiero, V., Nolè, G., Lanorte, A., Tucci, B., Cillis, G., & Murgante, B. (2022). Remote sensing and spatial analysis for land-take assessment in Basilicata Region (Southern Italy). *Remote Sensing*, *14*(7): 1692. DOI: https://doi.org/10.3390/rs14071692.

Secchi, D., Grimm, V., Herath, D.B., & Homberg, F. (2024). Modeling and theorizing with agent-based sustainable development. *Environmental Modelling & Software, 171*: 105891. DOI: https://doi.org/10.1016/j.envsoft.2023.105891.

Shivakumar, B.R. (2021) Land cover mapping capability of chaincluster, K-means, and ISODATA techniques—A case study. In *Advances in VLSI, Signal Processing, Power Electronics, IoT, Communication and Embedded Systems: Select Proceedings of VSPICE 2020*. Springer Singapore. DOI: https://doi.org/10.3390/rs14071692.

Talukdar, S., Singha, P., Mahato, S., Pal, S., Liou, Y.A., & Rahman, A. (2020). Land-use land-cover classification by machine learning classifiers for satellite observations—A review. *Remote Sensing*, *12*(7): 1135. DOI: https://doi.org/10.3390/rs12071135.

Tassi, A., & Vizzari, M. (2020). Object-oriented lulc classification in google earth engine combining snic, glcm, and machine learning algorithms. *Remote Sensing, 12*(22): 3776. DOI: https://doi.org/10.3390/rs12223776.

Tayyebi, A., & Pijanowski, B.C. (2014). Modelling multiple land use changes using ANN, CART and MARS: Comparing tradeoffs in goodness of fit and explanatory power of data mining tools. *International journal of applied earth observation and geoinformation, 28:* 102-116. DOI: https://doi.org/10.1016/j.jag.2013.11.008.

Teimouri, M.S., Forghani, A., & Baghban, S. (2022). A Geospatial Analysis Approach for Mapping and Ranking of Tourist Corridors in Mashhad Metropolis Iran. *World Journal of Geo-matics and Geosciences*, *2*(1): 1–23. DOI: 10.31586/wjgg.2022.240.

United Nations Department of Economic and Social Affairs. (2015). *Transforming our world: the 2030 agenda for sustainable development.*

Yu, Q., Wu, W., Yang, P., Tang, H., Zhou, Q., & Chen, Z. (2013). Progress of agent-based agricultural land change modeling: A review. *Shengtai Xuebao/Acta Ecologica Sinica*, *33*(6), 1690-1700.

Vahidi, H., & Yan, W. (2014). Towards spatially explicit agent-based model for simulation of informal transport infrastructure indirect growth dynamic in informal settlements. The International Archives of the Photogrammetry, *Remote Sensing and Spatial Information Sciences, 40:* 273-279. DOI: https://doi.org/10.5194/isprsarchives-XL-2-W3-273-2014.

Valbuena, D., Verburg, P.H., Bregt, A.K., & Ligtenberg, A. (2010). An agent-based approach to model land-use change at a regional scale. *Landscape ecology*, *25*: 185-199. DOI: https://doi.org/10.1007/s10980-009-9380-6.

Walker, R. (2004). Theorizing land-cover and land-use change: the case of tropical deforestation. *International regional science review, 27*(3): 247-270. DOI: https://doi.org/10.1177/0160017604266026.

Wang, Z., Lin, L., Zhang, B., Xu, H., Xue, J., Fu, Y., Zeng, Y., & Li, F. (2023). Sustainable urban development based on an adaptive cycle model: A coupled social and ecological land use development model. *Ecological Indicators, 154*: 110666. DOI: https://doi.org/10.1016/j.ecolind.2023.110666.

Wang, C., Zhan, J., & Xin, Z. (2020). Comparative analysis of urban ecological management models incorporating low-carbon transformation. *Technological Forecasting and Social Change, 159*: 120190. DOI: https://doi.org/10.1016/j.techfore.2020.120190.

Wang, S. Q., Zheng, X. Q., & Zang, X. B. (2012). Accuracy assessments of land use change simulation based on Markov-cellular automata model. *Procedia Environmental Sciences, 13*, 1238-1245. DOI: https://doi.org/10.1016/j.proenv.2012.01.117.

Wilensky, U. (1999). *NetLogo*. Center for connected learning and computerbased modeling, Northwestern University, Evanston. Available at: http://ccl.northwestern.edu/netlogo/.

Yousefi, S., Mirzaee, S., Almohamad, H., Al Dughairi, A. A., Gomez, C., Siamian, N., Alrasheedi, M., & Abdo, H. G. (2022). Image classification and land cover mapping using sentinel-2 imagery: optimization of SVM parameters. *Land, 11*(7): 993. DOI: https://doi.org/10.3390/land11070993.

Zhaka, L., & Xhina, E. (2021). Canada's Provinces Geospatial Data Visualization Using NetLogo and GIS. *International Journal of Scientific and Technological Research*, *7*.

Zarin, T., & Esraz-Ul-Zannat, M. (2023). Assessing the potential impacts of LULC change on urban air quality in Dhaka city. *Ecological Indicators, 154*:

110746. DOI: https://doi.org/10.1016/j.ecolind.2023.110746.

Zeraatpisheh, M., Ayoubi, S., Brungard, C.W., & Finke, P. (2019). Disaggregating and updating a legacy soil map using DSMART, fuzzy c-means and k-means clustering algorithms in Central Iran. *Geoderma*, *340*: 249-258. DOI: https://doi.org/10.1016/j.geoderma.2019.01.005.

Zhang, L., Han, R., & Cao, H. (2021). Understanding Urban Land Growth through a Social-Spatial Perspective. *Land, 10*(4): 348. DOI: https://doi.org/10.3390/land10040348.

Zhang, X., & Li, P. (2014). Lithological mapping from hyperspectral data by improved use of spectral angle mapper. *International Journal of Applied Earth Observation and Geoinformation, 31*: 95-109. DOI: https://doi.org/10.1016/j.jag.2014.03.007.

Zhang, W., & Wang, M.Y. (2018). Spatial-temporal characteristics and determinants of land urbanization quality in China: Evidence from 285 prefecture-level cities. *Sustainable Cities and Society, 38:* 70–79. DOI: https://doi.org/10.1016/j.scs.2017.12.011.

Zhao, L., Liu, X., Xu, X., Liu, C., & Chen, K. (2022). Three-Dimensional Simulation Model for synergistically simulating urban horizontal expansion and vertical growth. *Remote Sensing, 14*(6): 1503. DOI: https://doi.org/10.3390/rs14061503.

Zhao, M., Zhou, Y., Li, X., Cheng, W., Zhou, C., Ma, T., & Huang, K. (2020). Mapping urban dynamics (1992–2018) in Southeast Asia using consistent nighttime light data from DMSP and VIIRS. *Remote Sensing of Environment, 248*: 111980. DOI: https://doi.org/10.1016/j.rse.2020.111980.

CC BY NC